

Robust Reinforcement Learning Algorithm for Vision-based Ship Landing of UAVs

Vishnu Saj, Bochan Lee, Dileep Kalathil, and Moble Benedict

Abstract—This paper addresses the problem of developing an algorithm for autonomous ship landing of vertical take-off and landing (VTOL) capable unmanned aerial vehicles (UAVs), using only a monocular camera in the UAV for tracking and localization. Ship landing is a challenging task due to the small landing space, six degrees of freedom ship deck motion, limited visual references for localization, and adversarial environmental conditions such as wind gusts. We first develop a computer vision algorithm which estimates the relative position of the UAV with respect to a horizon reference bar on the landing platform using the image stream from a monocular vision camera on the UAV. Our approach is motivated by the actual ship landing procedure followed by the Navy helicopter pilots in tracking the horizon reference bar as a visual cue. We then develop a robust reinforcement learning (RL) algorithm for controlling the UAV towards the landing platform even in the presence of adversarial environmental conditions such as wind gusts. We demonstrate the superior performance of our algorithm compared to a benchmark nonlinear PID control approach, both in the simulation experiments using the Gazebo environment and in the real-world setting using a Parrot ANAFI quad-rotor and sub-scale ship platform undergoing 6 degrees of freedom (DOF) deck motion. [The video of the real-world experiments and demonstrations is available at this URL.](#)

I. INTRODUCTION

In recent years, there has been an increasing interest in developing autonomous control algorithms for UAVs for tracking a moving target and landing on it using only the camera sensor information for localization [1]–[4]. Developing such an autonomous algorithm for a vertical take-off and landing (VTOL) capable unmanned aerial vehicle (UAV) on a small moving ship, using only a monocular camera in the UAV for tracking and localization, is a particularly challenging task due to the small landing space, six degrees of freedom ship deck motion, limited visual references for localization, and adversarial wind gusts. The classical control approaches for this problem have been to use proportional-derivative (PD) control [3], [5], proportional-integral-derivative (PID) control [2], [6], linear quadratic regulator (LQR) [7]–[9], adaptive control [10]–[12], and model predictive control (MPC) [13]. While these approaches are partially successful in addressing the problem, they are often restricted to very specific settings due to three crucial weaknesses. First, the performance of the PD/PID type controllers solely depends on the design

of its gain parameters, which are typically difficult to fine-tune, especially in the simulator setting. PD/PID controllers have also limited transient response capabilities. Second, the MPC and LQR approaches often require a very sophisticated analytical model of the real-world UAV and obtaining such a model can be very challenging in practice. Moreover, for computational tractability, the design of the optimal control policies using these approaches is often limited to simplified settings such as linear policy and quadratic costs. Third, the classical control approaches are typically not robust against adversarial disturbances such as wind gusts and parameter mismatches/uncertainties between the simulator model and the real-world system model. These weaknesses often result in unsatisfactory performance in real-world settings. In this work, we propose a new autonomous control algorithm using the robust reinforcement learning approach in order to overcome these challenges and to achieve superior performance both in simulations and in real-world experiments.

Reinforcement Learning (RL) is an area of machine learning that addresses the problem of learning the optimal control policy for a stochastic dynamical system when its model is unknown. RL algorithms have seen impressive successes recently in a number of application such as playing games [14], [15] and robotics [16]–[19]. However, most of these successes are either in the simulation domain or in the structured real-world settings, which are significantly different from the challenging real-world setting such as the VTOL problem in the presence of adversarial wind gusts. Training RL algorithms in the real-world setting is infeasible because it can be catastrophic; for example, an undertrained policy may crash the drone. This challenge is typically overcome by training the RL controller in a simulator. However, it is very difficult to incorporate the diverse and complex real-world drone-environment interactions in a simulator. Moreover, the parameter mismatches between the simulator model and real-world environment cannot be accounted while training the RL control policies in a simulator. This leads to the problem known as *simulation-to-reality (sim-to-real) gap*, where the RL policies learned using a simulator may not perform well for the real-world setting. In this work, we overcome this challenge by developing a problem specific robust RL control policy and architecture by adapting the domain randomization approach [20]–[22] for the ship landing problem.

One integral component of any UAV algorithm capable of autonomous landing is a computer vision based algorithm for tracking the moving target and estimating the position of the UAV with respect to this target. Previous works used methods such as tracking the H/T-shaped landing marks, points, or

Corresponding author Vishnu Saj is with the Department of Aerospace Engineering, Texas A&M University, College Station, TX, 77840 USA e-mail: vishnu02saj@tamu.edu. This work has been funded by the Center for Unmanned Aircraft Systems (C-UAS), a National Science Foundation Industry/University Cooperative Research Center (IUCRC) under NSF award Numbers IIP-1161036 and CNS-1946890, along with significant contributions from C-UAS industry members.

lights on the deck [1], [4], [23], [24]. Methods involving visual tracking of deck motion is not ideal for VTOL capable UAVs because actively controlling the UAV to match the complex deck motion could excite unstable UAV attitude dynamics. This is even more unsafe when the aircraft is in close proximity to the moving deck because even a small control error can cause a catastrophic accident due to an impact by the deck. In this paper, we develop a computer vision based algorithm inspired by the practical ship landing procedure that navy helicopter pilots follow [25]–[28]. This procedure uses a gyro-stabilized (indicating the true horizon independent of ship motions) *horizon reference bar* as a visual cue. The pilot stabilizes the helicopter attitude using this visual cue and then commands vertical landing, agnostic of the deck motion. We develop a computer vision algorithm which detects this horizon reference bar, and continuously estimates the relative position of the UAV with respect to this horizon reference bar using only a monocular vision camera on the UAV.

Our main contribution are the following:

- We develop a robust reinforcement learning based control algorithm for autonomous vision-based ship landing of VTOL capable UAVs.
- We develop a computer vision based algorithm for estimating the relative position of the UAV with respect to the horizon reference bar using only a monocular vision camera.
- We demonstrate the superior performance of our algorithm in a real-world setting using a Parrot ANAFI quad-rotor and sub-scale ship platform undergoing 6 degrees of freedom (DOF) deck motions.

Related work: RL-based flight attitude control is discussed in [29]. An RL approach for UAV landing task on a moving platform using a variant of the DDPG algorithm is discussed in [30]. An actor-critic RL framework used to fly a UAV by following designated waypoints is presented in [31]. In [32], a variant of the DDPG algorithm is used to recover a UAV attitude quickly from an out-of-trim flight state. By leveraging a probabilistic model of drone dynamics, a model-based reinforcement learning strategy is used to control a quadrotor in [33]. Using an imitate-reinforce training framework, [34] proposed an end-to-end policy network for enabling a drone to fly through a tilted narrow gap. [35] used model-based reinforcement learning on a Crazyflie centimeter-scale quadrotor with rapid dynamics to predict and control on a low level. However, these works do not address the problem of designing RL controllers that are robust against adversarial disturbances such as wind gusts.

II. RELATIVE POSITION ESTIMATION USING MONOCULAR VISION CAMERA ON THE UAV

We develop a computer vision algorithm which first detects the horizon reference bar on the ship platform and then estimates relative position of the UAV with respect to this reference. The ship platform model with the horizon reference bar and the motion deck used in our real-world demonstration is shown in Fig. 1. As mentioned before, this



Fig. 1: Ship platform model with horizon reference bar and motion deck used in our real-world demonstrations.

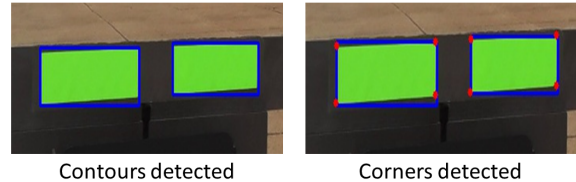


Fig. 2: Detecting the horizon reference bar.

approach of using horizon reference bar as the primary visual cue is motivated by the practical ship landing procedure that navy helicopter pilots follow [25], [28]. The relative position estimated by our computer vision algorithm is then used as part of the state information in the RL control algorithm.

A more detailed discussion of our relative position estimation approach is available in the technical report [36], which includes the details omitted from here due to page limit.

A. Image Filtering, Corner Detection and Screening

Our algorithm takes the monocular camera image captured by the UAV as input, and first performs a Hue-Saturation-Value (HSV) filtering to detect the green rectangles corresponding to the horizon reference bar. In the HSV filtered image, there may exist small white patches outside the rectangles and black voids inside the rectangles. We use the morphological opening technique to remove the white patches in the image and the morphological closing is used to fill up small voids in those rectangles. We then use the watershed algorithm [37] to obtain clear boundaries of the rectangles.

Once the green rectangles are isolated, the next goal is to detect the contours and corner points. To detect the eight corners precisely, our algorithm first find the contours of the detected region and bound it in rectangles as shown in Fig. 2. Thus, the size and shape of the detected areas are very close to the green rectangles, and the corners of those bounding rectangles can be used as rough estimates of the actual corners. We adapt the Förstner corner detection [38] method to detect the corner points of the rectangles based on the rough corners obtained by contour detection.

The algorithm then uses a screening procedure to ensure that no false corners are detected in the image. All the detected corners are sorted in a particular order, and a simple coordinate system is used to identify the height, width and the slope of different sides of the rectangles. Even though the detected regions are not perfect rectangles in the image,

the width and height of the rectangles have similar lengths and slopes. A $\pm 10\%$ tolerance level is set for the lengths and a $\pm 5\%$ tolerance level is set for the slopes.

B. Relative Position Estimation

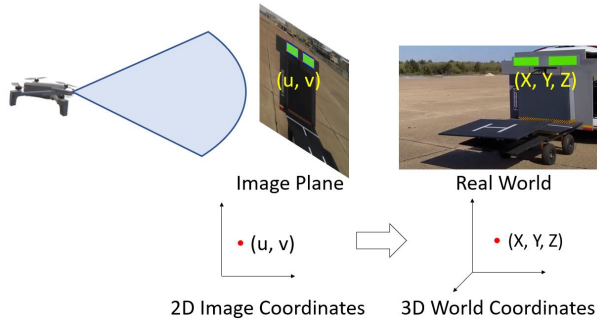


Fig. 3: Geometric relationship of 2D image coordinates and 3D real-world coordinates.

Our estimation is based on a single camera calibration method using a planar object [39], [40] and a conventional pinhole camera model is used to derive the geometric relation. Let (X, Y, Z) is a point on the visual cue and let (u, v) is the corresponding point on the image frame (pixel position in the image), see Fig. 3. Their correspondence is given by

$$s \begin{bmatrix} u \\ v \\ 1 \end{bmatrix} = \mathbf{A} \begin{bmatrix} \mathbf{R} & t \\ 0 & 1 \end{bmatrix}^{-1} \begin{bmatrix} X \\ Y \\ Z \\ 1 \end{bmatrix}, \quad (1)$$

where s is the scaling factor, \mathbf{A} corresponds to the intrinsic camera parameters, \mathbf{R} is the rotation matrix and t is the translation vector. Given a set of n 3D coordinates of an object and its corresponding 2D projections on the image, the Perspective-n-Point (PnP) algorithm can be used to determine the relative position and orientation. First, the PnP algorithm solves Eq.(1) to obtain the rotation matrix \mathbf{R} and the translation vector t . The PnP algorithm uses an iterative approach called Levenberg-Marquardt optimization [41], [42] to minimize the re-projection error. Once the \mathbf{R} matrix and t vector is computed, the UAV camera position with respect to the visual cue can be obtained as $[X_{\text{cam}} \ Y_{\text{cam}} \ Z_{\text{cam}}] = -\mathbf{R}^{-1}t$.

III. ROBUST REINFORCEMENT LEARNING BASED CONTROL ALGORITHM

A. Reinforcement Learning Preliminaries

We first give a brief overview of the Markov Decision Processes (MDP) and reinforcement learning terminologies.

An MDP can be defined as a four-tuple $(\mathcal{S}, \mathcal{A}, P, R)$, where \mathcal{S} is the state space and \mathcal{A} is the action space, $P(s'|s, a)$ is the probability of transitioning from state s to s' upon taking action a , and $R(s, a)$ is the reward. A control policy $\pi : \mathcal{S} \rightarrow \mathcal{A}$ specifies the control action to take in each possible state. The performance of a policy is measured using the metric of value of a policy, V_π , defined as $V_\pi(s) = \mathbb{E}_\pi[\sum_{t=0}^{\infty} \gamma^t R(s_t, a_t) | s_0 = s]$ where, $s_{t+1} \sim P(\cdot | s_t, a_t)$, $a_t = \pi(s_t)$, s_t is the state of the system at time t , and a_t is the action taken at time t ,

and $\gamma \in (0, 1)$ is the discount factor. The goal is to find the optimal policy π^* that achieves the maximum value, i.e., $\pi^* = \arg \max_\pi V_\pi$. The corresponding value function, $V^* = V_{\pi^*}$, is called the optimal value function. The optimal value function and policy satisfy the Bellman equation, $\pi^*(s) = \arg \max_a (R(s) + \sum_{s' \in \mathcal{S}} P(s'|s, a) V^*(s'))$.

When the system model P is known, the optimal policy can be computed using dynamic programming. However, in most real-world applications, the system model is either unknown or difficult to estimate precisely. Even if the model is known, directly computing the optimal nonlinear control policy is typically intractable for systems with large state and action spaces. RL offers a data driven and computationally tractable approach for learning the optimal control policy using only the trajectory samples generated from an offline simulator of the system.

Policy gradient algorithms are a popular class of RL algorithms for systems with continuous state and action spaces. In a policy gradient algorithm, we represent the policy as π_θ , where θ denotes parameters of the neural network that represents the policy. Let $J(\theta) = \mathbb{E}_s[V_{\pi_\theta}(s)]$, where the expectation is w.r.t. to a given initial state distribution. The goal is to find the optimal parameter $\theta^* = \arg \max_\theta J(\theta)$. This is achieved by implementing a gradient ascent update, $\theta_{k+1} = \theta_k + \alpha_k \nabla J(\theta_k)$, where α_k is the learning rate. The gradient $\nabla J(\theta)$ is given by the celebrated policy gradient theorem as $\nabla J(\theta) = \mathbb{E}_{\pi_\theta}[Q_{\pi_\theta}(s, a) \nabla \log \pi_\theta(s, a)]$, where expectation is w.r.t. the state and action distribution realized by following the policy π_θ . Here, Q_{π_θ} is the Q-value function corresponding to the policy π_θ . The Q-value function is also represented using a neural network (different from the one used for policy representation). There are many popular policy gradient algorithms such as TRPO [43], PPO [44], SAC [45]. In this work, we adapt the state-of-the-art twin delayed DDPG (TD3) algorithm [46] to develop a robust control policy for the VTOL problem.

B. VTOL UAV Control as an RL Problem

1) *Physical UAV and the Simulator Model:* For the real-world demonstration, we use Parrot Anafi [47], a commercial off-the-shelf quadrotor UAV. This particular UAV comes with a Gazebo simulator model which can be used for training the RL algorithm. Gazebo is a realistic simulation engine that is widely used for robotics applications [48]. The RL algorithm can communicate with the simulation engine using a framework called Olympe [49]. Olympe allows the control of UAV and access to its sensors through python scripts.

2) *State Space:* The relative position of the UAV w.r.t to the target (horizon reference bar) is used as part of the state. We also include the velocity of the UAV as a part of the state. The velocity can be obtained either directly from the corresponding sensor or simply by a numerical calculation from the current and past position states. We use the past five position and velocity measurements as the current state. More precisely, $s_t = (p_t, v_t, p_{t-1}, v_{t-1}, \dots, p_{t-5}, v_{t-5})$, where p_t and v_t are the relative position and velocity of the UAV w.r.t. the target in Euclidean coordinates.

3) *Action Space*: The Parrot Anafi drone we use has four different control actions: roll, pitch, yaw, and heave. During the experiments, we observed that the optimal roll and pitch actions heavily depend on the wind disturbances. Also, the main objective here is vertical landing. So, we consider only the roll (to move the UAV right or left) and the pitch (to move the UAV forward or backward) as the actions for the RL controller. For the Parrot Anafi drone, the roll and pitch action can be controlled independently. The roll controller objective is to achieve a certain target on the roll axis and maintain that position without considering the pitch motion. Similarly, for the pitch controller, the objective is to maintain a position on the pitch axis independent of the roll motion.

4) *Reward Function*: Designing the appropriate reward function that implicitly represents the underlying real-world task is one of the most important aspect for developing an RL algorithm for that real-world task. We use a carefully designed a reward function for our problem as given below.

$$\text{Reward} = \begin{cases} -\frac{1}{20}|a_{\text{diff}}| - \frac{1}{10}|a| & \text{if } |d| \leq 0.1 \\ & \text{(Region-1)} \\ -2|d| - \frac{1}{20}|a_{\text{diff}}| - \frac{1}{10}|a| & \text{if } 0.1 \leq |d| \leq 0.4 \\ & \text{(Region-2)} \\ -1 & \text{if } 0.4 \leq |d| \leq 2 \\ & \text{(Region-3)} \\ -(T_{\text{max}} - T_{\text{inside}}) & \text{if } |d| > 2 \end{cases}$$

The reward function is divided into four regions based on the value of d , which denotes the deviation along the x-axis for the pitch control case and the deviation along the y-axis for the roll control case. The reward function is normalized in the range $[0, -1]$. Region-1 is where the UAV is within 0.1 m of the target location. Since this is the preferred region for hovering, we impose only a action penalty. Here, a_{diff} is the difference between current action value and average of past five action values and a is the current action value. The penalization based on a_{diff} is to ensure that the control action trajectory is smooth while the penalization on a forces the controller to not select high control values when it is close to the target. In Region-2, which is between 0.1 m and 0.4 m from the target, we use a reward function based both on the distance from the target position and the control action. When d is between 0.4 m and 2 m, which is Region-3, we impose the maximum penalization irrespective of the control action and the deviation. The objective is that the UAV needs to get within the 0.4 m mark which is considered as safe zone for landing as quick as possible. We also want the algorithm to accumulate higher rewards (less negative) if it reaches the target point as early as possible and if it stays in the vicinity of the target. To ensure this, the final part of the reward is designed, where T_{max} is the maximum episode time during training and T_{inside} is the time that the UAV stays within 2 meters from the target. Our training episode ends when $|d| > 2$ and this terms kicks in only when a control action pushes the UAV outside of 2 meters.

5) *Robust RL through Domain Randomization*: One of the most challenging aspect of RL-based robotic control

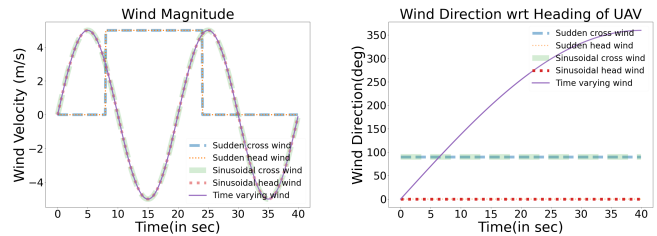


Fig. 4: Wind magnitude and direction in different scenarios.

design is the sim-to-real gap arising from using the control policy trained on a simulator in the real-world. There are inevitable mismatches between the simulator setting and real-world setting in the UAV control problem, not only due to the possible mismatches between the model parameter values of the simulator and real-world UAV, but also due to the presence of adversarial disturbances such as wind gust in the real-world. Domain randomization [20]–[22] is an approach for overcoming the sim-to-real gap by randomizing the simulator environment during the training of the RL control policy. We adapt the domain randomization approach to develop a UAV controller that is robust against adversarial wind gusts in the real-world environment.

During the RL training, we use the Gazebo simulation engine to generate multiple wind scenarios: constant magnitude wind (-10 m/s to 10 m/s), sudden wind magnitude change (-5 m/s to 5 m/s magnitude change), and a sinusoidal wind (amplitude of 5 m/s and time periods of 10 secs, 20 secs, 30 secs, 40 secs and 50 secs). We randomize the wind conditions (including its magnitude and directions) over the learning episodes. It is observed that headwind affects the forward drift and crosswind affects the sideward drift. Hence crosswinds are applied for roll controller training and headwinds are applied for pitch controller training.

The estimation of relative position and velocity using the vision system is prone to errors depending on how far the camera is located from the visual cue. So, we apply the domain randomization to the state estimation system also to be robust against this uncertainty. In addition to this, we also use domain randomization for being robust against issues due to time delays in the vision and control systems.

As mentioned before, we adapt the state-of-the-art TD3 algorithm for training an RL controller in the manner described above. The selected hyper-parameter are: $\gamma = 0.99$, policy delay = 2, learning rate = $1e-4$, buffer size = $1e5$. The system used for training is LENOVO Legion Y740-15IRH, which is composed of Intel(R) Core(TM) i7-9750H CPU with 2.60GHz, 2592 Mhz, 6 Cores, and 12 Logical Processors. It features an integrated NVIDIA GeForce GTX 1660 Ti 6GB Graphics and 8GB of LPDDR4 memory with a 128-bit interface. The system has Ubuntu 18.04 OS with Nvidia driver version 440 and CUDA version 10.2. The same system is used for flight simulations and testing.

IV. SIMULATION RESULTS

We evaluated the performance of our robust RL controller in the Gazebo simulation environment. We consider the

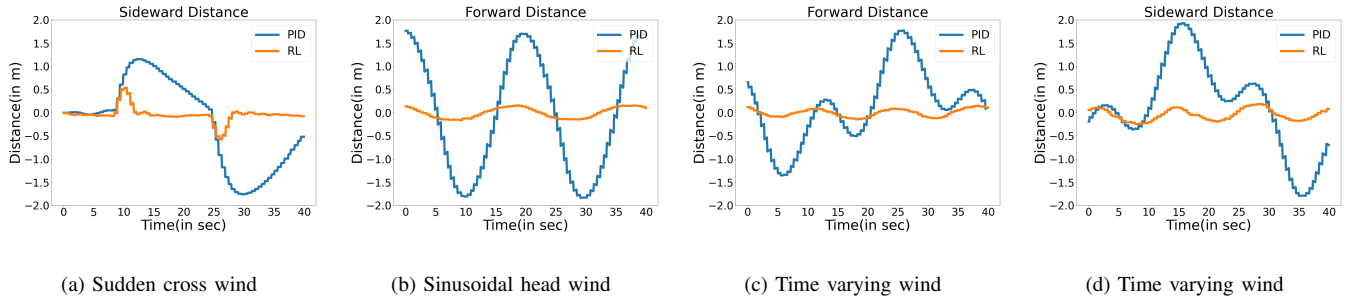


Fig. 5: Deviation from the desired position in different wind scenarios for the hovering task.

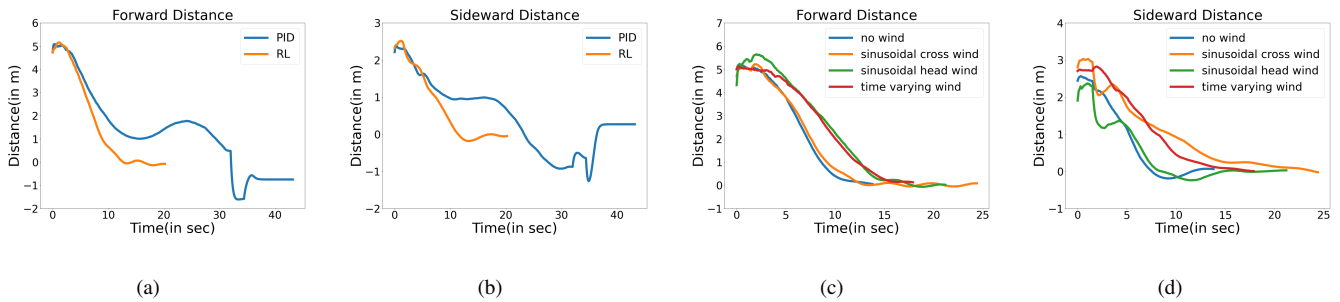


Fig. 6: Distance from the target position in different wind scenarios for the landing task.

hovering task where the goal is to hover over the target and landing task where the goal is to perform vertical landing on the target, despite the adversarial wind conditions present during these tasks. The different wind scenarios we considered in our evaluation is shown in Fig. 4. As a benchmark, we use a PID control based algorithm developed in our prior work, described in the technical report [36]. We show that our robust RL controller achieves superior performance compared to this PID controller benchmark.

A. Hovering task in different wind scenarios

Figure 5a shows the sideward deviation from the desired position of the UAV in the presence of a sudden cross wind (magnitude changes from 0 to 5 m/s at the 8 second mark). The maximum sideward deviation for our robust RL approach is only one-third of the deviation for benchmark PID controller. Moreover, our robust RL approach is able to return the UAV to the desired position in less than 2 seconds, while this took at least 15 seconds for the PID controller. Figure 5b shows the forward deviations in presence of sinusoidal head wind. The maximum forward deviation for our robust RL approach is less than 20 cm and it is only one-tenth of the deviation for the benchmark PID control. Figure 5c shows the forward deviation in a more challenging scenario where both the magnitude and direction of the wind change over time. The wind magnitude is a sinusoidal function with an amplitude of 5 m/s and a time period of 20 seconds. The wind direction also changes continuously from 0° to 360° in every 40 seconds. Here also, the maximum deviation for our RL approach is less than 20 cm and it is only one-tenth of the deviation for the benchmark PID

controller. Figure 5d shows the sideward deviation for the same time varying wind scenario.

B. Landing task in different wind scenarios

Figures 6a and 6b show the distance of the UAV from the target landing position as a function of time in the presence of a time varying wind scenario described in the above subsection. Note that both the sideward and forward distance converges to zero for our robust RL approach. At the same time, the benchmark PID control approach is not able to make a safe landing in this wind scenario. Figures 6c and 6d show that the robust RL controller comfortably makes landing in a number of wind scenarios.

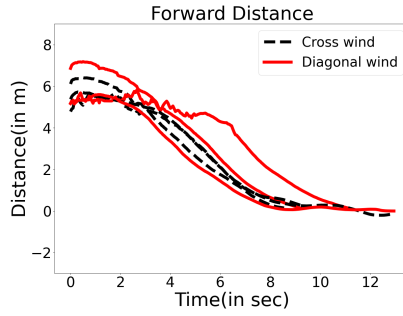
V. REAL-WORLD UAV DEMONSTRATIONS

A. Experimental Setup

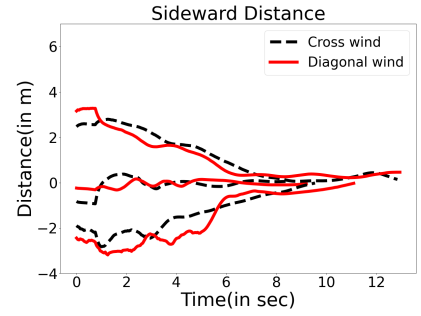
For the real-world demonstration, we use Parrot Anafi quadrotor UAV [47]. The schematic of the control system is shown in Fig. 8. The UAV has an embedded (onboard) inner-loop autopilot that controls the rotational speed of each propeller to achieve the commanded inputs generated by the outer-loop RL based control system (offboard). The UAV is controlled by a Python script that runs on an external computer which communicates with the UAV through the WiFi connection. The UAV transmits raw images captured by the onboard camera to the external computer in real-time, and the computer processes these images to provide estimates of relative position and other state variables. Based on the state estimate, the robust RL controller generates the roll and pitch control actions. The control actions are sent back



(a) Experimental Setup



(b) Forward Distance



(c) Sideward Distance

Fig. 7: Landing on stationary platform in different wind scenarios from different initial positions.

to the UAV, and the embedded inner-loop autopilot controls the rotating speed of each propeller based on the received control actions.

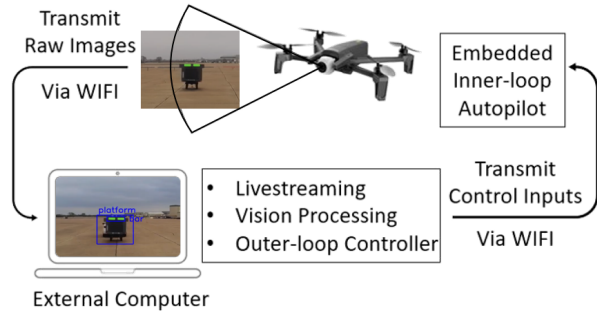


Fig. 8: Schematic of the UAV control.

We constructed a sub-scale ship platform model with horizon reference bar and motion deck for our real-world demonstration as shown in Fig. 1 and Fig. 7a. The width, height, and length of the ship platform are 5 ft, 5 ft, and 10 ft, respectively. The horizon bar always indicates a perfect horizon, and the motion deck has its own 6 DOF motions in addition to the forward translational motion, which is similar to what would be experienced on a real ship. We use a drum fan as shown in Fig. 7a for generating the wind gust. The fan can generate a wind gust with a maximum speed of 3 m/s (in low settings) and 5 m/s (in high settings).

B. Landing task experiment results

In our experiments, the UAV approaches the ship platform from different initial positions. We place the fan at two positions: at 90 degrees with respect to the trajectory of the UAV for generating a cross wind (as shown in Fig. 7a) and at 45 degrees with respect to the trajectory of the UAV for generating a diagonal wind (figure omitted due to page limit). The forward and sideward distance of the UAV as it approaches the landing platform is shown in Figs. 7b and 7c respectively. Figure 9 shows the landing spots on the platform for the same testing scenarios shown in Figs. 7b and 7c. As clear from these figures, our robust RL approach

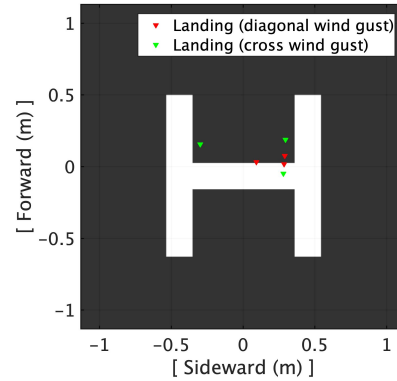


Fig. 9: Landing points on the platform for the different wind scenarios.

is able to land the UAV safely and smoothly on the platform in all scenarios.

The video of the real-world experiments and demonstrations is available at this URL.

VI. CONCLUSION

In this work, we addressed the problem of developing an algorithm for autonomous ship landing for VTOL capable UAVs in the presence of adversarial environmental conditions such as wind gusts. We first developed a computer vision based algorithm which uses the image stream from a single monocular vision camera in the UAV for estimating the relative position of the UAV w.r.t. a horizon reference bar on the landing platform. We then developed a problem specific robust RL algorithm by adapting the domain randomization approach that is capable of controlling the UAV to the landing platform even in adversarial wind conditions. We demonstrated the superior performance of our approach with respect to a benchmark PID control based approach by doing evaluations in simulations settings and in real-world settings. In our future, we plan to develop a robust meta-learning algorithm that can adapt to more diverse wind scenarios in real-time without compromising on the performance.

REFERENCES

- [1] J. L. Sanchez-Lopez, J. Pestana, S. Saripalli, and P. Campoy, "An approach toward visual autonomous ship board landing of a VTOL UAV," *Journal of Intelligent & Robotic Systems*, vol. 74, no. 1, pp. 113–127, 2014.
- [2] Q. H. Truong, T. Rakotomamonjy, A. Taghizad, and J.-M. Biannic, "Vision-based control for helicopter ship landing with handling qualities constraints," *IFAC-PapersOnLine*, vol. 49, no. 17, pp. 118–123, 2016.
- [3] W. K. Holmes and J. W. Langelan, "Autonomous ship-board landing using monocular vision," in *Proc. 72nd Am. Helicopter Soc Forum*, vol. 2, 2016, p. 36.
- [4] Y. Meng, W. Wang, H. Han, and J. Ban, "A visual/inertial integrated landing guidance method for UAV landing on the ship," *Aerospace Science and Technology*, vol. 85, pp. 474–480, 2019.
- [5] J. M. Daly, Y. Ma, and S. L. Waslander, "Coordinated landing of a quadrotor on a skid-steered ground vehicle in the presence of time delays," *Autonomous Robots*, vol. 38, no. 2, pp. 179–191, 2015.
- [6] O. Araar, N. Aouf, and I. Vitanov, "Vision based autonomous landing of multirotor UAV on moving platform," *Journal of Intelligent & Robotic Systems*, vol. 85, no. 2, pp. 369–384, 2017.
- [7] B. Lee, "Helicopter autonomous ship landing system," Master's thesis, Texas A&M University, 2018.
- [8] B. Lee and M. Benedict, "Development and validation of a comprehensive helicopter flight dynamics code," in *AIAA Scitech 2020 Forum*, 2020, p. 1644.
- [9] K. A. Ghamry, Y. Dong, M. A. Kamel, and Y. Zhang, "Real-time autonomous take-off, tracking and landing of UAV on a moving UGV platform," in *2016 24th Mediterranean conference on control and automation (MED)*. IEEE, 2016, pp. 1236–1241.
- [10] B. Hu, L. Lu, and S. Mishra, "Fast, safe and precise landing of a quadrotor on an oscillating platform," in *2015 American Control Conference (ACC)*. IEEE, 2015, pp. 3836–3841.
- [11] J. Kim, Y. Jung, D. Lee, and D. H. Shim, "Landing control on a mobile platform for multi-copters using an omnidirectional image sensor," *Journal of Intelligent & Robotic Systems*, vol. 84, no. 1, pp. 529–541, 2016.
- [12] K. Xia, S. Lee, and H. Son, "Adaptive control for multi-rotor UAVs autonomous ship landing with mission planning," *Aerospace Science and Technology*, vol. 96, p. 105549, 2020.
- [13] P. Vlantis, P. Marantos, C. P. Bechlioulis, and K. J. Kyriakopoulos, "Quadrotor landing on an inclined platform of a moving ground vehicle," in *2015 IEEE International Conference on Robotics and Automation (ICRA)*. IEEE, 2015, pp. 2202–2207.
- [14] V. Mnih, K. Kavukcuoglu, D. Silver, A. A. Rusu, J. Veness, M. G. Bellemare, A. Graves, M. Riedmiller, A. K. Fidjeland, G. Ostrovski *et al.*, "Human-level control through deep reinforcement learning," *nature*, vol. 518, no. 7540, pp. 529–533, 2015.
- [15] D. Silver, A. Huang, C. J. Maddison, A. Guez, L. Sifre, G. Van Den Driessche, J. Schrittwieser, I. Antonoglou, V. Panneershelvam, M. Lanctot *et al.*, "Mastering the game of go with deep neural networks and tree search," *nature*, vol. 529, no. 7587, pp. 484–489, 2016.
- [16] T. P. Lillicrap, J. J. Hunt, A. Pritzel, N. Heess, T. Erez, Y. Tassa, D. Silver, and D. Wierstra, "Continuous control with deep reinforcement learning," in *ICLR (Poster)*, 2016.
- [17] S. Levine, C. Finn, T. Darrell, and P. Abbeel, "End-to-end training of deep visuomotor policies," *The Journal of Machine Learning Research*, vol. 17, no. 1, pp. 1334–1373, 2016.
- [18] I. Akkaya, M. Andrychowicz, M. Chociej, M. Litwin, B. McGrew, A. Petron, A. Paino, M. Plappert, G. Powell, R. Ribas *et al.*, "Solving rubik's cube with a robot hand," *arXiv preprint arXiv:1910.07113*, 2019.
- [19] T. Haarnoja, S. Ha, A. Zhou, J. Tan, G. Tucker, and S. Levine, "Learning to walk via deep reinforcement learning," in *Robotics: Science and Systems*, 2019.
- [20] F. Sadeghi and S. Levine, "CAD2RL: real single-image flight without a single real image," in *Robotics: Science and Systems*, 2017.
- [21] J. Tobin, R. Fong, A. Ray, J. Schneider, W. Zaremba, and P. Abbeel, "Domain randomization for transferring deep neural networks from simulation to the real world," in *2017 IEEE/RSJ international conference on intelligent robots and systems (IROS)*. IEEE, 2017, pp. 23–30.
- [22] X. B. Peng, M. Andrychowicz, W. Zaremba, and P. Abbeel, "Sim-to-real transfer of robotic control with dynamics randomization," in *2018 IEEE international conference on robotics and automation (ICRA)*. IEEE, 2018, pp. 3803–3810.
- [23] G. Xu, Y. Zhang, S. Ji, Y. Cheng, and Y. Tian, "Research on computer vision-based for UAV autonomous landing on a ship," *Pattern Recognition Letters*, vol. 30, no. 6, pp. 600–605, 2009.
- [24] O. A. Yakimenko, I. I. Kaminer, W. J. Lentz, and P. Ghyzel, "Unmanned aircraft navigation for shipboard landing using infrared vision," *IEEE Transactions on Aerospace and Electronic Systems*, vol. 38, no. 4, pp. 1181–1200, 2002.
- [25] "Helicopter operations from ships other than aircraft carriers(hostac)," vol. I. NATO standard, 2017.
- [26] B. Lumsden, C. Wilkinson, and G. Padfield, "Challenges at the helicopter-ship dynamic interface," 1998.
- [27] J. Colwell, "Maritime helicopter ship motion criteria-challenges for operational guidance," *Challenges for Operational Guidance-NATO RTO Systems Concepts and Integration Panel SCI-120. Berlin, Germany*, 2002.
- [28] Aeronautical General Instruments Limited a portfolio company of AGI Holdings LLC, "Stabilised horizon bar reference systems."
- [29] W. Koch, R. Mancuso, R. West, and A. Bestavros, "Reinforcement learning for UAV attitude control," *ACM Transactions on Cyber-Physical Systems*, vol. 3, no. 2, pp. 1–21, 2019.
- [30] A. Rodriguez-Ramos, C. Sampedro, H. Bavle, P. De La Puente, and P. Campoy, "A deep reinforcement learning strategy for UAV autonomous landing on a moving platform," *Journal of Intelligent & Robotic Systems*, vol. 93, no. 1-2, pp. 351–366, 2019.
- [31] Y. Li, H. Li, Z. Li, H. Fang, A. K. Sanyal, Y. Wang, and Q. Qiu, "Fast and accurate trajectory tracking for unmanned aerial vehicles based on deep reinforcement learning," in *2019 IEEE 25th International Conference on Embedded and Real-Time Computing Systems and Applications (RTCSA)*. IEEE, 2019, pp. 1–9.
- [32] J. Hwangbo, I. Sa, R. Siegwart, and M. Hutter, "Control of a quadrotor with reinforcement learning," *IEEE Robotics and Automation Letters*, vol. 2, no. 4, pp. 2096–2103, 2017.
- [33] P. Becker-Ehmck, M. Karl, J. Peters, and P. van der Smagt, "Learning to fly via deep model-based reinforcement learning," *arXiv preprint arXiv:2003.08876*, 2020.
- [34] J. Lin, L. Wang, F. Gao, S. Shen, and F. Zhang, "Flying through a narrow gap using neural network: an end-to-end planning and control approach," in *2019 IEEE/RSJ International Conference on Intelligent Robots and Systems (IROS)*. IEEE, 2019, pp. 3526–3533.
- [35] N. O. Lambert, D. S. Drew, J. Yaconelli, S. Levine, R. Calandra, and K. S. Pister, "Low-level control of a quadrotor with deep model-based reinforcement learning," *IEEE Robotics and Automation Letters*, vol. 4, no. 4, pp. 4224–4230, 2019.
- [36] B. Lee, V. Saj, M. Benedict, and D. Kalathil, "Intelligent vision-based autonomous ship landing of VTOL UAVs," *arXiv preprint arXiv:2202.13005*, 2022.
- [37] M. Couprie and G. Bertrand, "Topological gray-scale watershed transformation," in *Vision Geometry VI*, vol. 3168. International Society for Optics and Photonics, 1997, pp. 136–146.
- [38] W. Förstner and E. Gülch, "A fast operator for detection and precise location of distinct points, corners and centres of circular features," in *Proc. ISPRS intercommission conference on fast processing of photogrammetric data*. Interlaken, 1987, pp. 281–305.
- [39] Z. Zhang, "Flexible camera calibration by viewing a plane from unknown orientations," in *Proceedings of the seventh IEEE international conference on computer vision*, vol. 1. IEEE, 1999, pp. 666–673.
- [40] N. Araki, T. Sato, Y. Konishi, and H. Ishigaki, "Vehicle's orientation measurement method by single-camera image using known-shaped planar object," *Int. J. Innov. Comput. Inf. Control*, vol. 7, no. B, pp. 4477–4486, 2011.
- [41] K. Levenberg, "A method for the solution of certain non-linear problems in least squares," *Quarterly of applied mathematics*, vol. 2, no. 2, pp. 164–168, 1944.
- [42] D. W. Marquardt, "An algorithm for least-squares estimation of non-linear parameters," *Journal of the society for Industrial and Applied Mathematics*, vol. 11, no. 2, pp. 431–441, 1963.
- [43] J. Schulman, S. Levine, P. Abbeel, M. Jordan, and P. Moritz, "Trust region policy optimization," in *International conference on machine learning*. PMLR, 2015, pp. 1889–1897.
- [44] J. Schulman, F. Wolski, P. Dhariwal, A. Radford, and O. Klimov,

“Proximal policy optimization algorithms,” *arXiv preprint arXiv:1707.06347*, 2017.

- [45] T. Haarnoja, A. Zhou, P. Abbeel, and S. Levine, “Soft actor-critic: Off-policy maximum entropy deep reinforcement learning with a stochastic actor,” in *International conference on machine learning*. PMLR, 2018, pp. 1861–1870.
- [46] S. Fujimoto, H. Hoof, and D. Meger, “Addressing function approximation error in actor-critic methods,” in *International Conference on Machine Learning*. PMLR, 2018, pp. 1587–1596.
- [47] Parrot, “Parrot anafi quadrotor UAV,” <https://www.parrot.com/us/drones/anafi>, 2022 (accessed Sep 15, 2022).
- [48] Open Robotics, “Gazebo simulator,” <https://gazebo.org/home>, 2022 (accessed Sep 15, 2022).
- [49] Parrot, “Olympe 7.3,” <https://developer.parrot.com/docs/olymppe/index.html>, 2022 (accessed Sep 15, 2022).